J. Fluid Mech. (1980), *vol.* 97, *part* 4, *pp.* 655–671
Printed in Great Britain

Extensional flow of dilute polymer solutions

By DAVID F. JAMES AND J. H. SARINGER
Department of Mechanical Engineering, University of Toronto, Canada

(Received 9 May 1979)

The behaviour of dilute polymer solutions in sink flow, viz., radial flow toward a point, was investigated experimentally and theoretically. Solutions of polyethylene oxide, in the drag-reducing concentration range, were pushed through a 60° conical channel at Reynolds numbers of order 10^2. Preliminary studies revealed a range of flow conditions in which the flow was free of secondary motion yet non-Newtonian effects were significant. Measurements of pressure differential between two radial positions yielded the non-Newtonian normal stress developed in the radial direction; the magnitude was the same order as the Newtonian stress, i.e., as the dynamic pressure $\frac{1}{2}\rho V^2$.

Several fluid models were analysed to determine the stress generated by each in sink flow. It was found that a solution of Rouse–Zimm flexible macromolecules produces a stress which is three orders of magnitude below the observed level, and that macromolecules with finite extension fall short by two orders. A suspension of elongated particles, of the type analysed by Batchelor, was also considered, but application to the present case was difficult because of the small scale required by the theory. Consequently, the theory was extended to include particles the size of the flow field, and an order-of-magnitude analysis revealed that for such particles to produce the desired stress, the aspect ratio must be $O(10^{\frac{3}{2}})$, and the cross dimension is likely $O(0{\cdot}1)\,\mu$m. Electron micrographs of freeze-dried samples of the polymer solutions showed the solute in the form of an irregular network of apparently undissolved strands, with diameters in the $O(0{\cdot}1)\,\mu$m range.

1. Introduction

Dilute polymer solutions are capable of exhibiting large non-Newtonian effects in a variety of flows. Probably the best known example is the reduction of wall shear stress by the addition of a few parts per million of a high molecular weight polymer. The additive alters the structure of the flow primarily in the viscous sublayer and buffer regions. There the molecules are believed to reduce unsteady elongational motions, thereby decreasing the transfer of momentum. Another situation in which large non-Newtonian effects are found is flow through a porous medium; comparably small amounts of polymer can increase the pressure gradient by a factor of order 10 (James & McLaren 1975). In this flow, a fluid particle is repeatedly stretched as it follows a tortuous path, and the increased hydraulic resistance is thought to be related to the fact that these fluids develop large normal stresses in extensional flow. The key fluid property, then, is extensional viscosity, or the ratio of this viscosity to the shear viscosity. The magnitude of this ratio has been determined by Metzner & Metzner

0022-1120/80/4431-8870 $02.00

(1970). Their work on dilute solutions of a polyacrylamide yielded values from $O(10^2)$ to $O(10^4)$ for this ratio, which is 3 for Newtonian fluids. Their measurements of extensional viscosity were found from flows through small orifices, in which the tensile stress was deduced from the measurement of jet thrust at the orifice exit.

The magnitudes reported by Metzner & Metzner depend significantly on the assumed form of the flow field upstream and downstream of the orifice, and the necessity of this assumption is typical of the problems encountered in making proper rheological measurements in extensional flow. In the first place, it is hard to devise experiments in which both the velocity field and the stress field are well defined. Also, as Ting & Hunston (1977) have noted, non-Newtonian behaviour is generated only when the deformation rate is sufficiently high and when the transit time at that rate is sufficiently long; in convective flow, these are conflicting requirements. Furthermore, high strain rates for dilute solutions can mean high Reynolds numbers, in which inertial effects may overwhelm non-Newtonian effects, or even lead to turbulence. These problems with inertia are generally avoided or diminished by having a small-scale geometry, of order 0·1–1 mm, which was the case in the Metzners' experiments, and which will be the case for the extensional flow experiments to be described in this paper.

The rheological study reported herein was an outgrowth from past experiments on laminar flows of dilute polymer solutions. For some years we have attempted to understand the mechanics of these fluids by conducting experiments in which large non-Newtonian effects were generated in well-defined laminar flows. One of these experiments was mentioned earlier – the flow through a porous medium. In that investigation, the media were packed beds of small uniform beads, and the fluids were $O(10)$ p.p.m. solutions of polyethylene oxide (Union Carbide's Polyox) in water. These conditions produce the abnormally high pressure drops mentioned in the first paragraph, and the basic question that arose from that and similar work was: how does such a small amount of solute produce such a large stress? Experiments by the Metzners and by Balakrishnan & Gordon (1975) have yielded the magnitude of the stress, but the source of the non-Newtonian effect is not discussed.

This work started off to examine flow through porous media, mainly to explain the high pressure gradients and, it was hoped, to identify the underlying physical mechanism. Our first investigation was flow through a similar but simpler geometry, an orifice. Orifice flows are known to produce effects comparable to flows in porous media (e.g. Balakrishnan & Gordon 1975), although there is the difficulty that non-Newtonian behaviour in orifice flows is always accompanied by a large upstream vortex ring, while no secondary motion has been observed in a porous medium (James & McLaren 1975). Thinking that geometry was a factor, we initially studied flows through orifices of various shapes. This study revealed the general features of dilute solution flow in converging channels, and led to the design of a rheometer having a well-defined extensional flow field. Data from the rheometer prompted the analysis of various fluid models in extensional flow, from solutions of flexible macromolecules to suspensions of elongated particles.

2. Initial studies

Past work by several groups on the flow of polymer solutions through sudden contractions indicates that the onset of non-Newtonian behaviour is accompanied by the

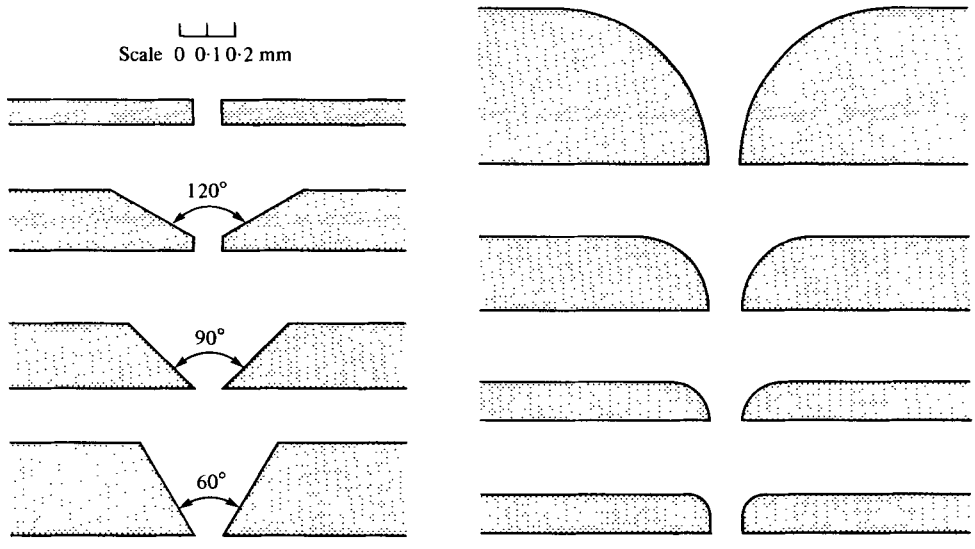

FIGURE 1. The various orifices tested in the preliminary study, shown to scale.

appearance of an upstream vortex ring. We first wondered if the sharp edge of the orifice promoted this secondary motion, remembering that no secondary motion was observed in a porous medium where the surfaces are well rounded. Consequently we tested a series of orifices of various shapes, all having a diameter at the minimum cross-section of about 0·1 mm. The shapes, shown in figure 1, were created by electrical discharge machining in plates of appropriate thickness. Each orifice plate was installed in a test chamber and fluid was driven through the orifice by a specially-designed roller pump, while the pressure drop across the orifice plate was monitored. The apparatus for the experiment is sketched in figure 2. By suspending micron-size mica flakes in the test fluids we were able to see, with the aid of a microscope, the gross features of the flow pattern within each channel as the flow measurements were taken. Water and dilute Polyox solutions, ranging from 10 to 100 p.p.m., were pushed through each orifice and, despite the variety in shape, the results for all orifices were remarkably similar. An example is presented in figure 3, for the 60° conical channel. At low flow rates, the pressure drop was the same as for water, and the observed streamline pattern was simple converging flow, as shown in inset (i). As the flow rate increased, the head suddenly jumped to several times the Newtonian value and secondary motion simultaneously appeared in the channel, of the form shown in inset (ii). This motion was a vortex ring which was usually highly asymmetric, highly unsteady and of large scale, extending well into the upstream reservoir. This irregular flow pattern and the increased pressure differential persisted as the flow rate continued to increase. While this behaviour was observed for all orifices, a different result was noted for very dilute solutions in a conical channel. Representative of this pattern are the 40 p.p.m. data in figure 3. The departure from water data occurred at about the same flow rate, but the deviation was gradual and the flow stayed in the pattern of inset (i). The head eventually increased to about twice the water value, the flow

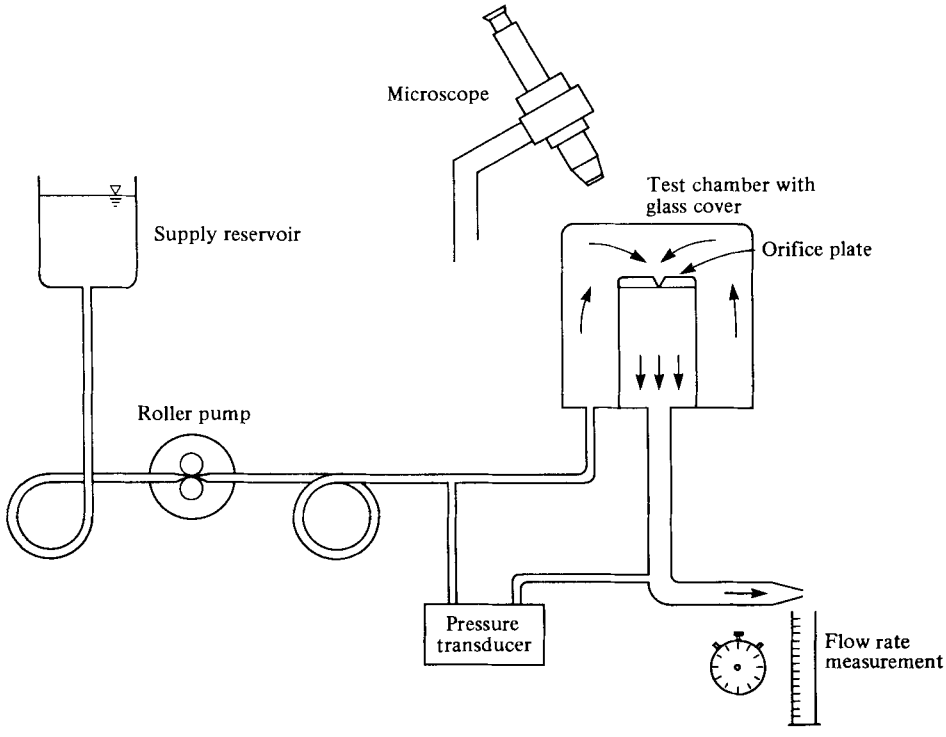

FIGURE 2. A schematic diagram of the apparatus for the orifice flow study and later for the sink flow measurements.

remaining free of secondary motion. Only at the highest flow rates did secondary motion appear, and then only by deliberately disturbing the flow.

These last data not only indicate a significant non-Newtonian effect but also suggest a method for measuring normal stresses. The Reynolds number of the flow, based on exit conditions, ranges from 30 at onset to a maximum of 300. At the upper end, the Newtonian and non-Newtonian contributions to the pressure differential are about equal, and so by some mechanism the solute produces a force competitive with inertia forces at a Reynolds number of 300. This is a very large force, especially when it is realized that the mechanism must, in the end, be dissipative in nature and hence this viscous effect due to the additive is $O(10^3)$ times that due to the solvent. The high Reynolds number also means that the core of the flow is free of shear, and consequently is virtually a sink flow. The boundary layer which forms along the channel wall has a thickness, relative to a cross dimension, of order $Re^{-\frac{1}{2}}$, which is $O(10^{-1})$ in the present case. Outside the boundary layer, the radial velocity is $Q/2\pi r^2(1-\cos\theta)$, where Q is the flow rate, r the radius from the apex, and θ the half-angle of the cone. With the deformation field well defined for the core of the flow, this channel is potentially useful for rheological work. However, the flow field downstream of the exit is uncertain even for Newtonian fluids, and so the reservoir-to-reservoir pressure differential does not correspond to a known velocity field. It would be preferable, of course, to measure the pressure just before the exit where sink flow still exists, and so a new channel was designed to meet this requirement.

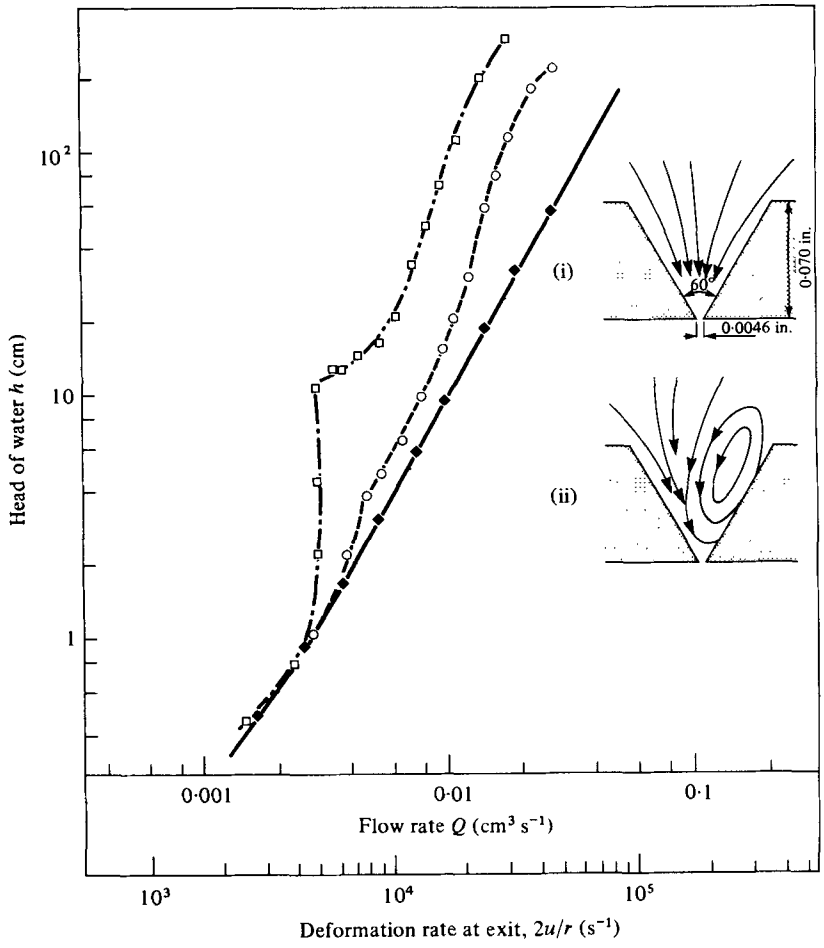

FIGURE 3. Measurements of head versus discharge for flow of water and dilute Polyox solutions through a 60° conical channel. For water (—◆—) and the 40 p.p.m. solution, (– –○– –), the flow pattern was simple converging flow as shown in inset (i). For the 80 p.p.m. solution (– ·—□–·–) the flow changed to the pattern shown in inset (ii) when the head increased rapidly. Data for the other 7 orifices in figure 1 were quite similar to the above results.

3. Measurement of pressure gradient in sink flow

Since the initial studies showed that a considerable non-Newtonian effect can be generated in a conical channel, a proper rheological experiment was designed on the basis of these findings. It was recognized that the flow Reynolds number must be $O(10^2)$ – high enough to create a virtual sink flow, but not be so high that viscosity-generated non-Newtonian effects are dominated by inertial forces and therefore hard to detect. A second requirement of the flow field is that the deformation rate be sufficiently high to generate departures from Newtonian behaviour. In sink flow, the strain rate is $2u/r$ where u is the radial velocity, and the data in figure 3 show that this parameter is $O(10^3)\,\mathrm{s}^{-1}$ at onset. (This order of magnitude has been found for other laminar flows of dilute polymer solutions and is often related to the largest relaxation time of the macromolecules.) The requirement that the deformation rate u/r be greater than $O(10^3)\,\mathrm{s}^{-1}$, and that the Reynolds number ur/ν be $O(10^2)$, means that the

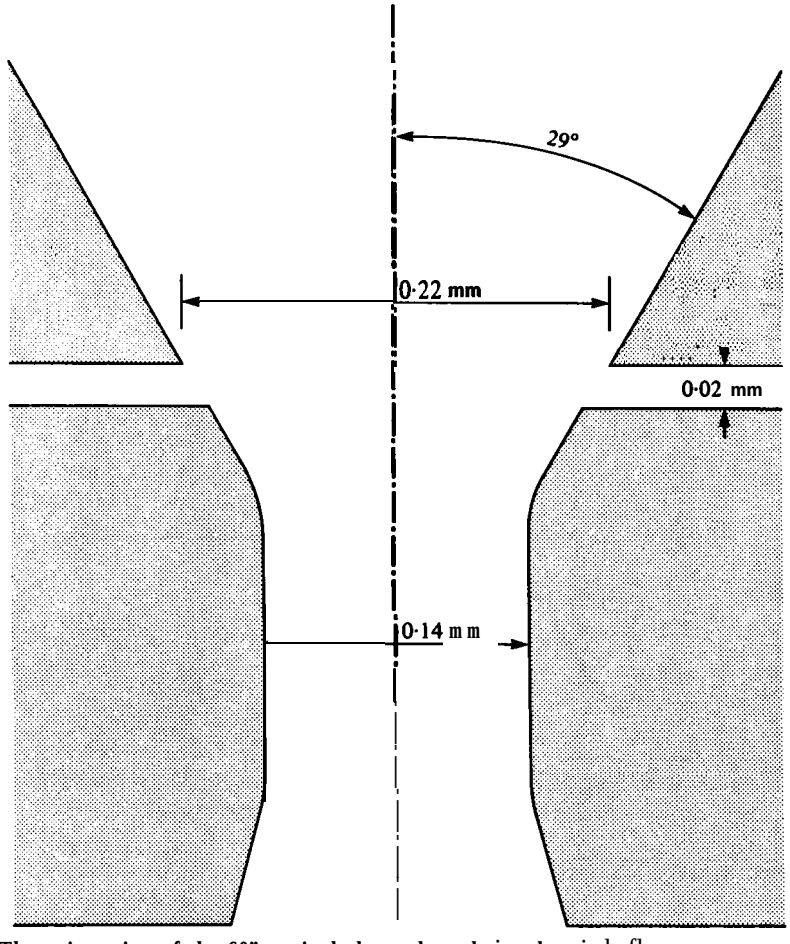

FIGURE 4. The exit region of the 60" conical channel used in the sink flow measurements. The pressure differential was measured between the 0·02 mm port and the upstream reservoir adjoining the channel, 2·5 mm from the apex.

exit radius must be less than $O[\nu/10]^{\frac{1}{2}}$. Since v is $0{\cdot}01\text{cm}^2/\text{s}^{-1}$ for our aqueous solutions, the exit radius must be less than about 0·3 mm. Consequently, a conical channel for sink flow studies has dimensions comparable to the channels in the initial studies.

Such a small exit radius makes it hard to locate a pressure port near the exit. As mentioned in the previous section, it is desirable to measure the pressure differential over a stretch where the flow is well approximated by sink flow. One port is naturally upstream; since the velocity goes as r^{-2}, the pressure decreases as r^{-4}, and thus it is only a short distance to a region that is effectively 'far upstream'. The other port must be located as close to, but upstream of, the exit, for the deformation rate is largest there, and the streamlines are still rays. If the port were further upstream, a faster flow rate would generate a deformation rate comparable to that at the exit, but this flow would create high enough normal stresses at the exit that secondary flow would likely be induced. Since the smallest port we could create was a slit of 0·02 mm width, the location was a compromise: it was close to the exit where the deformation rates are large and it was far enough upstream that the pressure variation over its width was

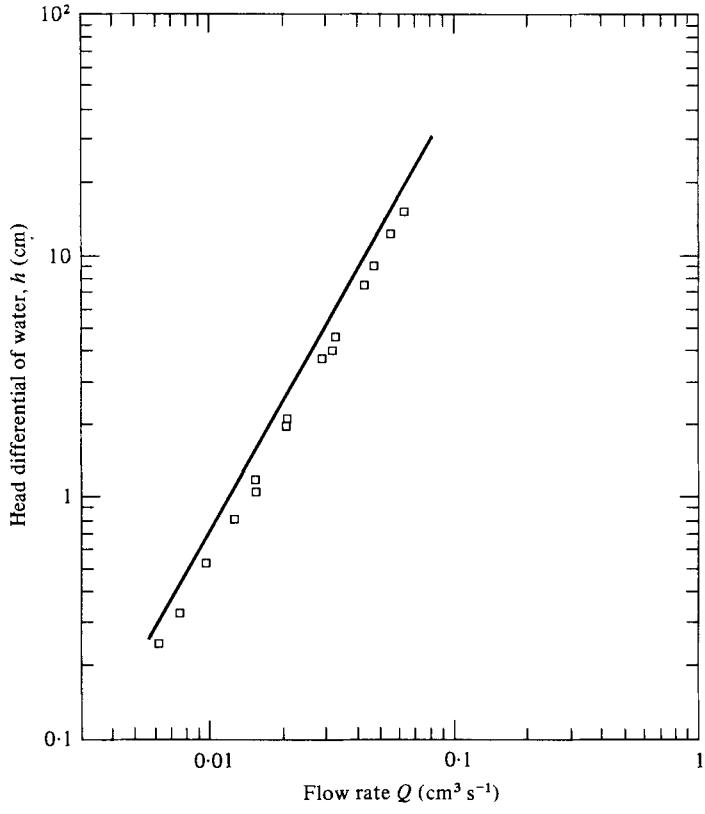

FIGURE 5. Head versus discharge for water flow in the conical channel of figure 4. The theoretical curve (——) is given by equation (1) in the text; □, experimental.

small. The geometry of the channel in the exit region is shown in figure 4; the full channel size, as measured from the apex to the upstream reservoir, is 2·5 mm.

The channel was installed in the test apparatus of figure 2. As fluids were pumped through the channel at known flow rates, the pressure differential between the port and the upstream reservoir was measured. The first measurements were for water and, for this Newtonian fluid, the relation between flow rate Q and head h can be estimated using the known similarity solution for axisymmetric flow. From the analysis in Rosenhead (1963), page 427, and using the numerical data from table V. 4 of the same reference, the $h-Q$ relation is found to be

$$Q = 2\pi r^2(2gh)^{\frac{1}{2}}(1-\cos\theta)\left[1-0{\cdot}415\left(\frac{2\nu}{r(2gh)^{\frac{1}{2}}}\right)^{\frac{1}{2}}\frac{\sin\theta}{1-\cos\theta}\right]. \tag{1}$$

This equation has the form

$$Q_{\text{actual}} = Q_{\text{inviscid}}\left[1-\frac{\text{constant}}{Re^{\frac{1}{2}}}\right],$$

showing that viscous effects diminish in the usual fashion as $Re^{-\frac{1}{2}}$. This relation is the solid line in figure 5, and the points are our water data. There is a constant discrepancy of about 20 % between the two, and the most likely source of error is in the value substituted for r. In fact, r was estimated from the 0·22 mm cross-dimension shown in

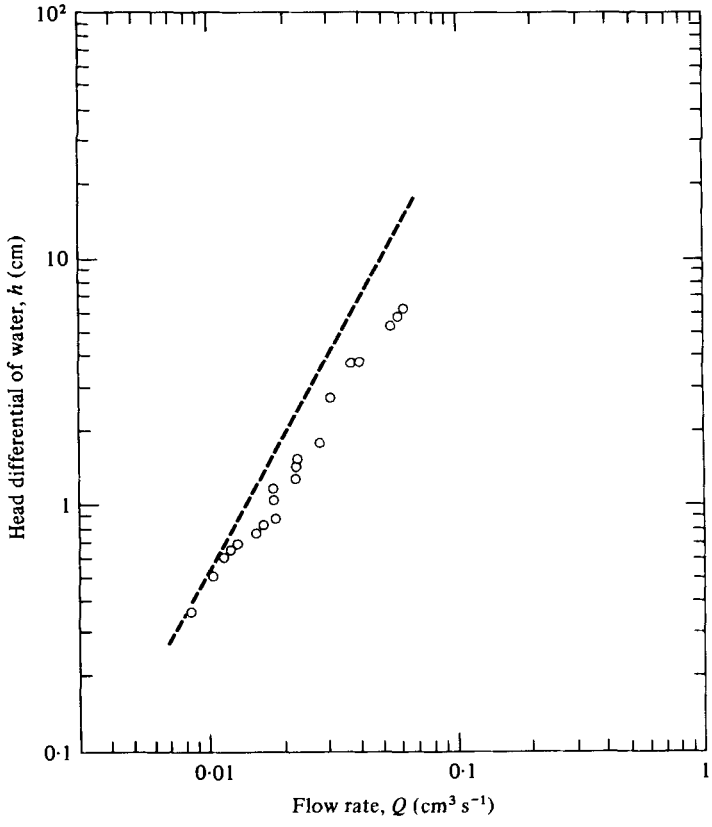

FIGURE 6. Head versus discharge for a 20 p.p.m. solution of polyethylene oxide in the conical channel (○). The dashed line represents the experimental data for water from figure 5.

figure 4, and this distance was difficult to measure to better than 10 % accuracy. In any case, the absolute values of the water data are not crucial, since their main purpose is to serve as a base line against which to compare the non-Newtonian data. A 20 p.p.m. solution of Polyox FRA was tested in the channel and the data are presented in figure 6. Onset occurs at about 0·01 cm^3 s^{-1}, a value which corresponds to a strain rate (at exit) close to the exit strain rate in figure 3. Unlike figure 3, however, the solution data in figure 6 fall *below* the water line. This result initially baffled us, for it was hard to conceive how any non-Newtonian mechanism could reduce the pressure below the value due to inertia alone. This situation was cleared up when we examined the relation between pressure and stresses for an anisotropic fluid.

4. The stress field

When a Newtonian fluid contains dissolved or suspended material, an additional stress σ'_{ij} may be generated. In this case, the constitutive equation for the medium may be expressed as:

$$\sigma_{ij} = -p\,\delta_{ij} + 2\mu\, e_{ij} + \sigma'_{ij}.$$

When the additional stress is in the radial direction and designated σ'_{rr}, then the three normal stresses in spherical coordinates become

$$\sigma_{rr} = -p + 2\mu\frac{du}{dr} + \tfrac{2}{3}\sigma'_{rr},$$

$$\sigma_{\phi\phi} = -p + 2\mu\frac{u}{r} - \tfrac{1}{3}\sigma'_{rr},$$

$$\sigma_{\theta\theta} = -p + 2\mu\frac{u}{r} - \tfrac{1}{3}\sigma'_{rr},$$

which satisfies the requirement that the bulk pressure is the negative of the mean normal stress. Hence the pressure measured by the port in the conical channel is larger than the Newtonian value by $\frac{1}{3}\sigma'_{rr}$. This means that the pressure difference between the port and far upstream is lower for non-Newtonian fluids, and thus explains why the data for the polymer solution fall below the water data in figure 6.

The non-Newtonian data from the channel flow indicate that σ'_{rr} is significant, and in the next section a number of fluid models are examined to find out under what conditions each could produce the observed magnitude of this stress.

5. Models for non-Newtonian fluids and their behaviour in sink flow

Dilute solutions may be represented by a variety of fluid models, and in this section we investigate several candidates which are capable of producing the non-Newtonian behaviour found in the experimental work. Since the results from the conical channel are essentially qualitative in nature, this analytical investigation will be of a similar nature, with many estimates made only to an order of magnitude.

(i) *Rouse–Zimm theory*

We first consider the classical Rouse–Zimm model for a dilute solution of flexible macromolecules. In this model, the polymer chain is represented by a series of beads and springs, and its dynamical behaviour has been found for a variety of flows. Recently, King (1977) solved the deformation of the bead-spring model in sink flow and found that the stress due to the molecules is

$$\sigma'_{rr} = O(1)\, c[\eta]\left(\tau_1\frac{du}{dr}\right)^{\frac{1}{3}}\mu\frac{du}{dr},$$

where c is the solute concentration, $[\eta]$ is the intrinsic viscosity, and τ_1 is the largest Rouse relaxation time. The corresponding Newtonian stress at high Reynolds numbers is the dynamic pressure $\frac{1}{2}\rho u^2$ and thus the ratio of non-Newtonian to Newtonian stresses, denoted nN/N, is

$$\frac{nN}{N} = O(1)\frac{c[\eta]}{Re}(\Gamma\tau_1)^{\frac{1}{3}}.$$

where Γ has been substituted for the strain rate. τ_1 is $O(10^{-3})$ s for high weight Polyox and Γ, calculated at the pressure port, is about $2\times10^4\,\mathrm{s}^{-1}$ at the highest flow rate; hence the maximum dimensionless strain rate $\Gamma\tau_1$ is about 20. Also, from the experiment, $[\eta]$ is $2500\,\mathrm{cm}^3\,\mathrm{g}^{-1}$, c is $20\times10^{-6}\,\mathrm{g\,cm}^{-3}$, and Re is about 300 at the port.

Consequently nN/N is $O(10^{-3})$, which is three orders below what was observed. A solution of Rouse–Zimm macromolecules, therefore, is not capable of generating the stresses measured in the channel.

(ii) *Molecules with finite extension*

King also found the stress field when the macromolecules have limited extension (private communication, 1977). He assumed that polymer chains deform initially as Rouse–Zimm macromolecules, but when the deformation reaches a prescribed value, the molecules are 'frozen' and remain in that configuration as they continue in sink flow. The molecules could be immobilized by entanglements or by crystallization, but this model was not intended to be associated with a particular physical mechanism; rather, it was intended to be a simple yet useful means of assessing the significance of finite extension. Since inextensible particles dissipate more energy than flexible ones, their effect on the flow is expected to be larger. King showed that the addition stress due to frozen extended macromolecules is

$$\sigma'_{rr} = \tfrac{2}{5}c[\eta]\left(\frac{l}{l_0}\right)^2 \mu \frac{du}{dr},$$

where l is the length of the molecule in extension and l_0 is its original length. Deformation begins when the strain rate exceeds τ_1^{-1}, and is assumed to occur upstream at r_1. The maximum effect is realized when the molecule locks just as it reaches the pressure port, at r_2. The maximum possible extension between r_1 and r_2 is that of a material line element, and its length increases by $(r_1/r_2)^2$. Hence $(l/l_0)^2$ for the molecules is $(r_1/r_2)^4$ at most. This ratio can also be expressed using Γ, the strain rate at the port. Since strain rate varies as r^{-3}, then nN/N for this case is

$$\frac{nN}{N} = \frac{3}{2}\frac{c[n]}{Re}(\Gamma\tau_1)^{\frac{4}{3}}.$$

This ratio is 20 times higher than the preceding case, and thus the non-Newtonian forces are still two orders too small. Other models of finite extension are available, but none will produce any stronger effects. Therefore we rule out the possibility that the observed stresses can be due to randomly-coiled molecules with finite extension.

(iii) *Small-scale long fibres*

Since macromolecules of any deformability cannot generate stresses to the levels measured in the experiment, it is necessary to consider a different type of model for the fluid. A logical candidate, after a solution of molecules, might be a suspension of particles. It is well known that particles which are round or nearly so generate an increase in viscosity which is the same order as the volume concentration. A very much larger effect is sought here, of the type possible with long particles. Recently, Batchelor (1971) found the stress developed by a suspension of elongated particles in pure straining motion. Brownian motion was neglected and the particles were aligned in a parallel but random array in the straining field. Batchelor showed that a considerable non-Newtonian effect is possible in a dilute concentration when the rod aspect ratio is large, and when the separation distance between rods is much larger than the rod

thickness but much smaller than the rod length. Specifically it was predicted that the additional stress in the straining direction is

$$\sigma'_{11} = \frac{4}{3}\frac{\phi}{\log(\pi/\phi)}\left(\frac{l}{b}\right)^2 \mu e_{11},$$

where ϕ is the volume concentration, l the particle half-length, b the effective radius, and e_{11} the strain rate in the principal direction, viz., $e_{22} = e_{33} = -\frac{1}{2}e_{11}$. When the flow is sink flow instead of pure straining, it is readily shown that the analogous stress is

$$\sigma'_{rr} = \frac{4}{3}\frac{\phi}{\log(\pi/\phi)}\left(\frac{l}{b}\right)^2 \mu \frac{du}{dr}$$

and then

$$\frac{nN}{N} \approx \frac{\phi}{\log(\pi/\phi)}\left(\frac{l}{b}\right)^2 \frac{1}{Re}.$$

The specific gravity of polyethylene oxide is close to 1, and assuming the density is the same down to the molecular level, ϕ is the same order as c, namely $O(10^{-5})$. Without an *a priori* value for l/b, we can instead work backwards from the known value for nN/N; that is, since nN/N is $O(1)$, the required aspect ratio l/b is $O(10^{\frac{7}{2}})$. The theory cannot yield any further information about the size of the particles, but a fundamental assumption in the theory limits the long dimension. The assumption is that the particle length is small compared to the dimensions of the flow field. For the conical channel, the characteristic length is the exit diameter 0·14 mm. Accordingly, $l \ll O(0{\cdot}1)$ mm and thus $b \ll O(10^{\frac{5}{2}})$ Å, which means that the cross dimension b must be $O(10)$ Å or less. This is the same order as the diameter of the molecular chain. From our previous discussion of molecular extension, it is difficult to conceive how a molecular chain or a group of chains, originally randomly-coiled far upstream, could be stretched out to the extent that the effective aspect ratio is $O(10^{\frac{7}{2}})$ at the channel throat.

(iv) *Large-scale long fibres*

Although the Batchelor theory is limited to particles of molecular dimensions, it does suggest that elongated particles – perhaps with much larger dimensions – could account for the non-Newtonian effects. Consequently, a revised theory was developed for 'large-scale' particles in sink flow, particles whose length may be comparable to the size of the flow field. This theory, which has been set aside in the appendix, shows that the stress for large-scale particles is

$$\sigma'_{rr} = \frac{\phi}{\log(\pi/\phi)}\left(\frac{l}{b}\right)^2 g\left(\frac{r}{l}\right)\mu\frac{du}{dr},$$

which is similar to the relation governing small-scale particles except for the function $g(r/l)$. The exact form of g is given in the appendix, but since it is $O(1)$, then the order-of-magnitude arguments for l/b are the same as the previous case. Therefore the required aspect ratio l/b is still $O(10^{\frac{7}{2}})$ and, again, additional information is needed for estimates of l and b. First, it should be noted that our solutions are optically clear, and so the cross dimension of a suspended particle (assuming particles are in fact present) cannot be larger than about 1 μm. As for length, perhaps a realistic estimate is the size of the flow field; if the length were smaller, the small-scale theory would apply

and, if larger, then there should be some macroscopic evidence. Consequently, l is most likely of order 0·1 mm and the corresponding cross-dimension b would then be $O(0{\cdot}1\,\mu\text{m})$ or less.

This order-of-magnitude analysis shows that the most suitable model for our non-Newtonian fluid is a suspension of elongated particles, probably of the size of the flow field. If the solute actually has the form of particles or any equivalent configuration, such sizes should be detectable by standard instruments and techniques. Accordingly, we turned to an electron microscope to provide some clue as to the structure of the solute.

6. Electron microscopy of freeze-dried samples

We originally thought that molecular strands might be formed by the strong extensional motion in the converging channel, similar to what happens in shear-induced crystallization for more concentrated solutions (e.g. Pennings, van der Mark & Kiel 1970). Since such strands would remain intact for some time after leaving the elongational flow field, our idea was to capture this formation by quickly freezing a liquid sample. A small drop of the solution was allowed to fall into a pool of liquid nitrogen (−196 °C). The frozen sphere was removed to a vacuum chamber, the water was sublimated, and the deposit left on the container was examined in a scanning electron microscope.

Shown in figures 7 (*a*, *b*) (plate 1) are electron micrographs of the 20 p.p.m. Polyox solution from the sink flow experiments. Little difference was found between samples from the upstream and downstream reservoirs, and the sample in figure 7 is from the upstream chamber. Figure 7 (*a*) shows that the polymer residue has a mesh-like form, with strands of various lengths and diameters. At the larger magnification in figure 7 (*b*) the smallest diameter is about 0·1 μm, which was the cross-dimension estimated in the previous section for large-scale particles. Samples of other drag-reducing polymers were prepared in the same way and they too formed highly irregular networks; as an example, figure 7 (*c*) displays the formation from a 50 p.p.m. solution of polyacrylamide from Stockhausen. These photographs confirm the earlier pictures of fibrous structure by Ouibrahim (1978), at magnifications up to 230 times. Our use of the electron microscope permits a more accurate characterization of the structure, particularly to estimate the diameter of the smallest strands.

At first glance, there appear to be too many strands for a solution in which the weight fraction of the solute is only 20 parts per million. It must be remembered, however, that whatever the form of the solute, it collapses to a more compact form when the water is withdrawn. As a check, we estimated the total volume of strands from a series of micrographs covering the area of the residue. This was found to be comparable to the solute volume known from the concentration and drop size.

The micrographs suggest that the polymer does not dissolve to discrete molecules but remains in undissolved strands. It is not clear how the strands develop but it is doubtful that they are the product of the freeze-dry preparation. The time of freezing is estimated to be around 0·1 s, a factor of 10^2 higher than the relaxation time of the molecule. It is unlikely that a randomly-coiled chain in a stationary solvent would extend itself so much and so quickly, simply due to a drop in temperature. Nor is the drying technique likely to produce the strands. When the water molecules sublimate,

polymer segments will tend to bind to one another: a random coil will collapse to a sphere and fibre-like material will tend to ball up or link to form a three-dimensional mesh. The coalescence will certainly not produce strands or links from what were originally coils. The coalescence, however, may account for the fact that no ends were found for the strands in the micrographs. In fact, for the moment, there is no way of knowing if the observed network came from the solution or was formed during sublimation.

The existence of strands is wholly contrary to the accepted concept of discrete macromolecules in dilute solution. Since light-scattering has shown that high molecular weight polymers, including Polyox (Shin 1965), have a random-coil configuration in dilute solution, it is difficult to explain how strands could be present. Part of the answer lies with the fact that solutions prepared for light scattering are thoroughly mixed and then filtered. These steps will break up any network which may be present and will promote the dissolution of strands. Following a common practice, our method of preparing a solution for experiment is to first make a master solution and then prepare a dilute solution from it. Stirring of both solutions is always gentle so as to avoid 'degradation', and the dilute solution is generally used within days after preparation. This method of preparation appears to produce the strands, for when we intentionally degraded a solution by intense shearing, it no longer produced non-Newtonian effects, and its micrograph showed clumps and not fibres.

The concept of strands in solution has been suggested by other workers in addition to Ouibrahim. Sternberg, Lagerstedt & Lindgren (1977) found polymer strings when a concentrated solution was mixed with additional solvent, and went on to speculate that the polymer forms thin strands in the final stages of dissolution. Hinch & Elata (1979) proposed that stringy networks are formed when 'fresh' dilute solutions are prepared from concentrated master solutions. With such a model, they explain various non-Newtonian effects in laminar and turbulent flows and, in fact, cite the present work as supporting evidence.

7. Discussion of results

This work shows that a dilute solution of a high molecular weight polymer can behave hydrodynamically as a suspension of long fibres, and that the fibres may be slowly-dissolving microscopic strands of the solute. A number of points require clarification if the fluid is to be treated as a suspension. One concerns strand length. The suspension theory in § 5 showed that the particle aspect ratio must be $O(10^{\frac{1}{2}})$ to account for the non-Newtonian effects, but the strands observed in the micrographs – that is, the components of the mesh – have ratios nowhere close to this magnitude. The mesh is thought to be formed during the preparation of the solution and is envisaged to be continuous throughout the solvent. As such, it has no inherent length scale, but an effective length can be created by a flow field. When the fluid is stagnant, as in the upstream reservoir, the mesh fibres are thought to be randomly oriented. Once the solution is flowing, viscous drag alters the configuration of the network, and at sufficiently high flow rates Brownian motion forces are negligible and the strands are aligned primarily in the flow direction. Under these conditions, the mesh produces effects similar to a suspension of aligned long fibres and so a suspension model for the solution is quite appropriate. The critical strain rate for alignment is evident from the

data in figure 6 and turns out to be close to that for discrete flexible molecules (we can find no explanation for this similarity and believe it to be coincidental). At higher flow rates, critical straining occurs upstream of the exit and the effective length of the mesh is then the distance from this point to the exit. The maximum flow rate is about 10 times that at onset, and since the strain rate varies as r^{-3}, critical straining occurs at a radius about twice (viz. $10^{\frac{1}{3}}$) the exit radius. Hence the effective length for the mesh is the order of the exit radius, which was argued earlier as the appropriate size for large-scale particles.

The present findings are useful in understanding some flows of dilute polymer solutions, particularly flow through porous media. The very high pressure differentials in those media, mentioned in § 1, are almost certainly due to solute strands, for flexible macromolecules produce non-Newtonian effects which are just too small. The network concept also explains the 'degradation' observed in the porous media experiments; that is, the high pressure losses dropped off in the flow direction (James & McLaren 1975). It was thought then that degradation is due to molecular scission, but it may be that the porous medium breaks up the network and promotes mixing and dissolution of the strands. The fluid becomes more and more like a true solution as it proceeds through the porous medium, and non-Newtonian behaviour correspondingly tapers off.

Our results may also be relevant to drag reduction, but it is too early to be other than speculative. Certainly the solutions prepared for pipe friction experiments are similar to those prepared here, and degradation is noted in those flows too. Furthermore, Batchelor's (1971) theory is a convincing argument that some form of long particles are necessary to produce non-Newtonian effects which can compete with inertial forces near the wall. These long particles may be solute strands or they may be the molecules themselves, for there is a fair body of evidence showing that friction reduction occurs with bona fide solutions. Also Hinch (1977) has shown that a polymer molecule is stretched out by a strong flow and that it readily remains in extended form. Yet there is no direct evidence that molecules are extended in turbulent flow. So while long particles are likely necessary for drag reduction, the question remains as to what they are and how they are created.

This work was aided by constructive discussions with Dr E. J. Hinch of the University of Cambridge. The financial support by the National Research Council of Canada is also gratefully acknowledged.

Appendix. Stress generated by a suspension of large-scale elongated particles in sink flow

A key assumption in Batchelor's (1971) theory for elongated particles is that the particle length is small compared to the dimensions of the flow field. This restriction is necessary not only for statistical homogeneity in a small region but also for the assumed form of the flow field around the particle; that is, for small particles the external velocity with respect to the particle varies linearly as the distance from the particle centre. For longer particles, these premises are no longer valid and the analysis must be reworked. The reworking is done in this appendix and, to differentiate size, these longer particles are termed large-scale particles, even though the theory will be shown

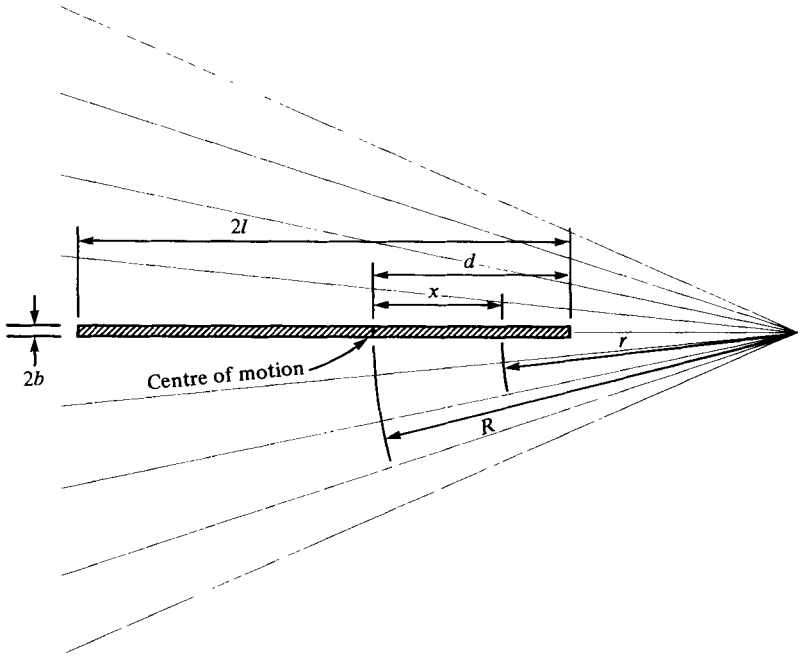

FIGURE 8. Definition sketch.

to apply to the Batchelor régime as well. Here, as in Batchelor's work, forces due to Brownian motion are ignored and thus the particles readily become aligned in the flow direction. In sink flow, the alignment is along rays, and consequently the particles will be straight regardless of their length and flexibility (a feature not possible in other flows of large-scale particles). Our particles, then, may be rods or flexible fibres, for the dynamics will be the same.

Following Batchelor's notation, the particles will be characterized as rods of length $2l$ and radius b. The rods are assumed to be the same length and to be distributed randomly in the flow field. The approach here is to analyse the force on a single rod from this to determine the normal stress due to a small concentration of such rods.

Dynamics of a single rod

The force per unit length exerted on an aligned rod by the fluid is

$$F = \frac{2\pi\mu}{\log(h/b)} V_r,$$

where V_r is the local relative velocity and $h(\gg b)$ is the effective distance between particles (Batchelor 1971). Unlike small-scale particles, the relative velocity at the centre of the rod cannot be assumed to be zero. Some point closer to the apex, where the net drag force is zero, will move with the local fluid velocity. Let this centre of motion (C.M.) be a distance R from the origin and a distance d from the end, as indicated in the sketch above (figure 8). The unperturbed fluid velocity u is A/r^2 where A is

proportional to the flow rate. At a distance x from the C.M., the relative velocity is $u(R-x)-u(R)$ or

$$V_r = \frac{A}{R^2}\frac{2Rx-x^2}{(R-x)^2}.$$

The tension T_c developed at the C.M. is

$$T_c = \int_0^d F\,dx = \frac{KA}{R^2}\frac{d^2}{R-d},$$

where

$$K = \frac{2\pi\mu}{\log(h/b)}.$$

Even though the rods are not parallel, h/b is a fixed ratio because the volume concentration ϕ is a constant and independent of r. Since h/b is well approximated by $(\pi/\phi)^{\frac{1}{2}}$ (Batchelor 1971), K is equivalent to $4\pi\mu/(\log\pi/\phi)$.

A similar analysis on the forces upstream of the C.M. yields

$$T_c = \frac{KA}{R^2}\frac{(2l-d)^2}{R+2l-d}.$$

Equating the two expressions for T_c yields the location of the C.M., viz.,

$$d = R+l-(R^2+l^2)^{\frac{1}{2}}.$$

The tension at any station x is

$$T(x) = \frac{KA}{R^2}\left(\frac{d^2}{R-d}-\frac{x^2}{R-x}\right), \quad -(2l-d) \leqslant x \leqslant d,$$

or, as a function of r (which will be more useful later),

$$T(r) = KA\left(\frac{d^2}{R^2(R-d)}-\frac{1}{r}\left(\frac{r}{R}-1\right)^2\right), \quad R-d \leqslant r \leqslant R+2l-d.$$

Computation of normal stress

In a sink flow, a spherical cap of radius r will slice through a number of suspended rods, and the tension in each rod will contribute to the extra normal stress σ_{rr} at that radius. The tension in a single rod is a random function for it depends where it is sliced. Since all positions along the rod are equally likely, the probability of slicing the rod between r and $r+dr$ is $dr/2l$. If the corresponding tension is $T(r)$, then the sum of all probable tensions yields the average tension T_1 for one rod, i.e.

$$T_1 = \frac{1}{2l}\int_{R-d}^{R-d+2l} T(r)\,dr.$$

If there are n rods intersecting the spherical cap per unit area, then the total tension per unit area is nT_1, which is just the extra stress σ_{rr}. The number n is related to the volume concentration ϕ by finding the volume of segments of n rods located in a thin layer of fluid adjacent to the spherical cap, viz, $\phi = n\pi b^2$. Hence

$$\sigma_{rr} = \frac{\phi}{\pi b^2 2l}KA\int_{R-d}^{R-d+2l}\left(\frac{d^2}{R^2(R-d)}-\frac{1}{R}\left(\frac{r}{R}-1\right)^2\right)dr.$$

After some manipulation and substitution for d, the integral reduces to

$$G(S) = \ln\frac{s+2}{s-2} - \frac{s}{2}\ln\frac{s^2}{s^2-4} - \frac{2}{s},$$

where $s = r/l$. It is apparent that the lower limit for s is 2, which restricts $2l$ to less than r and thus ensures that no rod extends beyond the apex. The stress is then

$$\sigma_{rr} = \frac{\phi}{\log(\pi/\phi)}\left(\frac{l}{b}\right)^2 \mu\frac{2A}{r^3}s^3 G(s),$$

which is similar to Batchelor's results for small-scale particles. In fact, since small particles are not excluded by the present theory, the above expression should reduce to the small-scale result for $l \to 0$. This is equivalent to $s \to \infty$, and for this limit $s^3 G(s)$ approaches $\frac{4}{3}$, the same coefficient as in Batchelor's work.

The remaining concern is the magnitude of σ_{rr} when l is very large, of order r. The appropriate limiting case is $s \to 2$, and for this limit $s^3 G(s) \to 8(\ln 4 - 1) \simeq 3$. Thus the order of magnitude of σ_{rr} depends only weakly on the scale of the particles.

REFERENCES

Balakrishnan, C. & Gordon, R. J. 1975 *A.I.Ch.E. J.* **21**, 1225.

Batchelor, G. K. 1971 *J. Fluid Mech.* **46**, 813–829.

Hinch, E. J. 1977 *Phys. Fluids* **20**, 22–30.

Hinch, E. J. & Elata, C. 1979 *J. Non-Newt. Fluid Mech.* **5**, 411–425.

James, D. F. & McLaren, D. R. 1975 *J. Fluid Mech.* **70**, 733–752.

King, D. H. 1977 M.A.Sc. thesis, University of Toronto.

Metzner, A. B. & Metzner, A. P. 1970 *Rheological Acta* **9**, 174–181.

Ouibrahim, A. 1978 *Phys. Fluids* **21**, 4–8.

Pennings, A. J., van der Mark, J. M. A. A. & Kiel, A. M. 1970 *Kolloid-Z. & Z. Poly.* **237** (2), 336–358.

Rosenhead, L. 1963 *Laminar Boundary Layers.* Oxford Press.

Shin, H. 1965 Sc.D. thesis, Massachusetts Institute of Technology.

Sternberg, L.-G., Lagerstedt, T. & Lindgren, E. R. 1977 *Phys. Fluids* **20**, 5276–5279.

Ting, R. Y. & Hunston, D. L. 1977 *J. Appl. Poly. Sci.* **21**, 1825–1833.

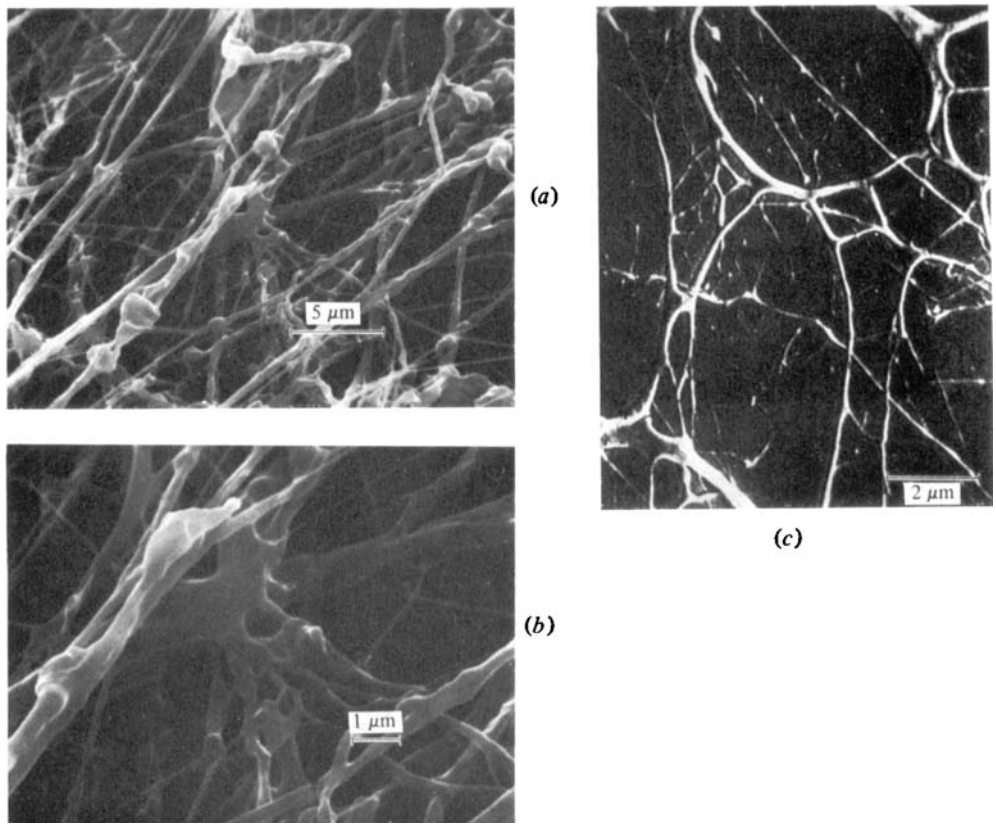

FIGURE 7. Electron micrographs of the residue from freeze-dried samples of dilute polymer solutions, the magnification being indicated by the scale in each photograph. (*a*) the 20 p.p.m. solution of polyethylene oxide from the sink flow experiments; (*b*) the same solution at a larger magnification, showing the size of the smallest strands; (*c*) a 50 p.p.m. solution of polyacrylamide from Stockhausen.